

Calcium Deficiency Diagnosis in Maize Leaves Using Imaging Methods Based on Texture Analysis

Fernanda de Fátima da Silva Devechio¹, Pedro Henrique de Cerqueira Luz¹, Liliane Maria Romualdo¹, Valdo Rodrigues Herling¹, Mário Antônio Marin¹, Odemir Marinez Bruno² & Álvaro Gómez Zuñiga²

¹ Department of Animal Science, Faculty of Animal Science and Food Engineering, University of Sao Paulo, Pirassununga, SP, Brazil

² São Carlos Institute of Physics, Department of Physics, University of São Paulo, Sao Carlos, SP, Brazil

Correspondence: Fernanda de Fátima da Silva Devechio, Department of Animal Science (ZAZ), Faculty of Animal Science and Food Engineering, University of Sao Paulo (FZEA/USP), Duque de Caxias Norte, 225, Jardim Elite, Pirassununga, SP, CEP: 13635-900, Brazil. Tel: 055-19-3565-4174. E-mail: ferdefatima@usp.br

Received: January 20, 2014

Accepted: January 29, 2022

Online Published: February 15, 2022

doi:10.5539/jas.v14n3p181

URL: <https://doi.org/10.5539/jas.v14n3p181>

This study is part of project 2010/18233-3 of the FZEA/USP and IFSC/USP. It was supported by FAPESP.

Abstract

The artificial vision system (AVS) uses image analysis methods that can interpret images and identify nutritional deficiency symptoms in plant, even in the early stages of development. The objective of this study was to propose methods of image processing using analysis by texture to identify the deficiency of calcium (Ca) in maize (*Zea mays* L.) plants grown in nutrient solution. Plants were grown in nutrient solution in a greenhouse. Calcium doses were 0.0; 1.7; 3.3 and 5.0 mM of Ca, with four replications. Plant and leaf images were sampled at three main stages of maize development: V4 (plants with four leaves fully developed), V6 (plants with six leaves fully developed) and V8 (plants with eight leaves fully developed). Sampled material was split into (i) index leaf (IL) of the growing stage (V4 = leaf 4, V6 = leaf 6, and V8 = leaf 8), and (ii) new leaf (OL), both to image capture and chemical analysis. Such leaves were scanned, processed by the AVS and chemically analyzed. The texture methods used by the AVS to extract deficiency characteristics in the leaf images were: Volumetric Fractal Dimension (VFD), Gabor Wavelet Energy (GWE) and VFD with canonical analysis (VFDCA). The amount of Ca in the solution resulted in variation in the concentration of Ca in NL and IL, allowing the observation of typical symptoms of Ca deficiency. The AVS method was able to identify all Ca levels in leaves, being the GWE the best indicator using color images, scoring 80% of rights in images of the middle section of new leaves in V4.

Keywords: artificial vision system, Gabor Wavelets, nutrient solution, greenhouse, *Zea mays* L.

1. Introduction

The world maize (*Zea mays* L.) production was 1162 million tons during the 2020/2021 crop season. The United States was responsible for 31% of that amount with average 10.8 ton ha⁻¹, China cropped 22.4% (6.3 ton ha⁻¹) and Brazil 8.9% with average 5.7 ton ha⁻¹ (FAO, 2022). To realize all its productive potential, the maize crops requires that nutrient supply (Amaral Filho et al., 2005) be adequate (Rambo et al., 2004). Symptoms of calcium (Ca) deficiency in maize results in internervous chlorosis and necrosis in younger leaves and tissues, reducing the cells stability and integrity, and growth is inhibited (Epstein & Bloom, 2006; Taiz & Zeiger, 2010; Marschner, 2011). The evaluation of nutritional state of the plants is usually done through chemical analysis or visual evaluation (Romualdo et al., 2014). Leaf chemical analyses of the nutrient status of the plant are time consuming and expensive Reis et al. (2006). In addition, the identification of the deficiency using leaf chemical analyses imply sampling at advanced phenological stage, which does not allow to take remediation actions for the crop (Wu et al., 2007). The visual diagnosis is a practical and quick method to investigate the nutrient deficiency in the plant, although its precision is limited and subjected to the experience of the observer (Baesso et al., 2007). The difficulties of evaluating the nutritional status of in maize plants on the same crop cycle are the motivation to propose additional approaches in nutrients (Luz et al., 2018). Since the chemical and visual diagnosis of

nutrient deficiency have such disadvantages, the artificial vision system (AVS) may become an efficient method to early identification of plant nutrient deficiency. The AVS can apply various methods to extract information from scanned images. The AVS is a computing system that can compare the images with a data bank in an automatic or semi-automatic routine (Punam & Udupa, 2001). The use of image analysis in agriculture is not recent and several previous examples of success are available. Lukina et al. (2001) estimated vegetation coverage in wheat (*Triticum aestivum* L.) using digital images. Karcher and Richardson (2003) used digital image analysis to determine the lawn color. Baesso et al. (2007) and Baesso et al. (2012) used image analysis and remote sensing techniques to identify nitrogen (N) deficiency in bean (*Phaseolus vulgaris* L.) plants using neural networks and were able to identify the deficiency level. Florindo et al. (2014) studied brachiaria species identification using imaging techniques based on fractal descriptors, and made possible the correct prediction of species in more than 93% of the samples. Silva et al. (2014) identified magnesium (Mg) deficiency in maize grown in a greenhouse and found a 75.5% of rights in the V4 stage, considered worthy trust through the Kappa index (Kappa = 0.9). Romualdo et al. (2014) used of artificial vision techniques for diagnostic of nitrogen nutritional status in maize plants, with percentage of right of 82.5 and 87.5% at V4 and V7, respectively, by Gabor Wavelet technique with color images. Luz et al. (2018) studied boron deficiency precisely identified on growth stage V4 of maize plant using texture image analysis, and achieved 88.75% of accuracy in differentiating between leaves using Fractal 3D, in V4 stage. Romualdo et al. (2018) used spectral indexes for identification of nitrogen deficiency in maize, and found accuracy rate for N patterns was 80% at V4 stage and 93% at V7 stage. Baesso et al. (2020) studied artificial vision for nutritional diagnosis of corn grown with calcium silicate and magnesium and found a 66% of rights. Patricio and Riederb (2018) reviewed the computer vision and artificial intelligence in precision agriculture for the five most produced grains in the world: maize, rice, wheat, soybean, and barley and concluded that Computer vision systems can be used in grading systems for maize and provides accurate descriptive data. It was identified that there are gaps to be filled with the development of artificial intelligence for automation of tasks in the field. The use of methods capable to precisely identify the nutrient status of plants is an excellent tool to manage maize nutrition, allowing to supply fertilizer in the same crop cycle, which is not possible using the present day human visual diagnosis and/or leaf chemical analysis.

The objective of this study was to propose methods of image processing using analysis by texture to identify the deficiency of calcium (Ca) in maize (*Zea mays* L.) plants grown in nutrient solution, using an AVS of different leaf sections.

2. Method

2.1 Greenhouse Experiment

The maize (*Zea mays* L.), hybrid DKB 499 was grown in a greenhouse using a hydroponic system with two plants per 3.6 L pot, in nutrient solution. Maize was sown in plastic trays filled with clean sand and kept there up to two weeks. Deionized water was supplied. Plants were then moved to the solution pots, supported by a foam layer in such a way that their roots were immersed in the nutrient solution. The nutrient solution was based on the Hoagland & Arnon (1950) formulation at 50% and with adaptation for the Ca levels. After five days, solution in the pots were brought 100% of the formulation. Solutions were replaced at each week. The pH was monitored and kept between 5 and 6 and temperature averaged at 28 °C. Each pot had their own bubbling system which worked for 10 seconds at each 30 seconds interval.

The levels of Ca were: 0.0; 1.7 (33% of full dose); 3.3 (66% of full dose) and 5.0 mM (of full dose—100%) of Ca. Plant and leaf images were sampled at three stages of maize development: V4 (plants with four leaves fully developed), V6 (plants with six leaves fully developed) and V8 (plants with eight leaves fully developed). According to Fancelli (1986), at stage V4 occurs the definition of the productive potential, at V6 the definition of the number of seeds in the ear, and at V8 the definition of the number and size of the ear.

Sampled material was split in shoot, roots, new leaf (NL) and index leaf (IL) of the growing stage (V4 = leaf four; V6 = leaf six, and V8 = leaf eight). NL and IL to image capture and chemical analysis. For chemical analysis, all material was washed, dried in an oven with air circulation at 65 °C, grind and saved in plastic bags for further nutrient analyses, according to methodology described in Bataglia et al. (1983). Samples were solubilized with nitric-perchloric acid for determination of Ca in IL and NL.

2.2 Experimental Design

Experimental design was fully random in a 4x3 factorial (four Ca levels and three sampling events) with four replications. In each collecting period established, 16 pots were sampled (samples destructive).

2.3 Statistical Analysis

Statistical data analysis was accomplished using analysis of variance and Tukey test at 5% probability. Such analysis was applied to data from Ca concentration in plants (g kg^{-1}), shoot dry mass (g plant^{-1}) and roots dry mass (g plant^{-1}). According to Steel et al. (1997) the statistical model used was as follows:

$$Y_{ijk} = m + E_i + N_j + EN_{ij} + e_{ijk} \quad (1)$$

Where, Y_{ijk} is the value measured in the unit subjected to treatment ij at replication k , m is the overall average of the experiment; E_i is the effect of maize stage of development; N_j is the effect of Ca levels applied; e_{ijk} is the effect of uncontrolled factors at the unit subjected to treatments ij at replication k .

In cases where the F test was significant ($p \leq 0.05$) for interaction between Ca levels and stages of plant development, the unfolding had the objective to study the levels inside the effect of maize stage of development. In such cases, one regression analysis was performed to each development stage (three in total).

2.3 Artificial Visual System

The images were processed by artificial vision, using the traditional four steps approach: acquisition, image segmentation, feature extraction and classification / identification (Bruno, 2000; Gonzalez & Woods, 2007).

2.4 Acquisition

The first step of the analysis is the digitalization (acquisition) of the leaf. Scanned leaves were IL and NL (the first leaf to show Ca deficiency). The leaves IL and NL were cut from the plant, digitalized using a conventional table-scanner (HP Scanjet 3800), and stored in uncompressed digital format. The high resolution and the uncompressed storage allow for the windowing-based approach in which small leaf epidermal structures are analyzed. Subsequently, the images were stored in TIFF extension for further processing and extraction of windows by the methods of artificial vision presented below and subsequently classified.

2.5 Image Segmentation

On the image segmentation, the digitalized image is processed in order to be analyzed by the system. The segmentation process was used to discard the image background and artifacts (damages, holes, etc.) and also to isolate target areas which showed nutrient deficiency symptoms (Rossatto et al., 2011).

2.6 Feature Extraction

This step consists of two parts. On the first, the leaves' images are split and segmented from the background, after that they are oriented (down to top). On the second part, there are extracted windows (areas of interest on the image) from the leaves, which are used on the next step. The feature extraction step is responsible for the analysis of the windows. For each window, a signature is extracted in order to characterize the leaf.

Three sectors of each scanned leaf were used: bottom, middle and top (Figure 1), for IL and NL, summing up 50 color images and 50 gray images for each. The sub-images can be called windows and they are sampled from different positions of the leaf, discarding leaf defects as damages and holes, according to Casanova et al. (2009) and Rossatto et al. (2011).

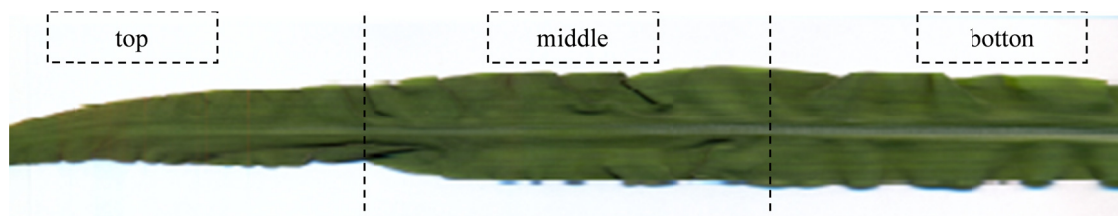


Figure 1. Separation of leaves for image analysis considering 3 parts: bottom, middle and top

In each part of the leaf were extracted windows with 80×80 pixel of the leaf surface. Each window was oriented horizontally and stored in uncompressed format. The leaf texture windowed technique was proposed in Casanova et al. (2009). The main idea of the approach is analyzing the leaf micro-texture, this way, the 80×80 pixel windows can isolate the micro-texture features, allowing that the macro-texture does not interfere into the texture analysis. Beside that, as showed in Rossatto et al. (2011) the windowed approach allows to extract samples for different

positions of the leaf and allow discard windows that are completely different of homogeneous regions, that could contain out layers, such as leaf defects, insect bitten among others.

A texture descriptor is used to extract a numeric vector that represents the sub-image in the feature space. On the last step, a pattern classification scheme separates the feature space to classify the samples. Different texture methods were used separately to demonstrate our proposal. The methods used were Volumetric Fractal Dimension (VFD), Gabor Wavelet (GW) and Volumetric Fractal Dimension with canonical analysis (VFDCA). These methods were chosen based on the good results obtained in the leaf texture analysis. In Luz et al. (2018), Romualdo et al. (2018), Silva et al. (2014), Romualdo et al. (2014), Backes and Bruno (2013), Rossatto et al. (2011) and Backes et al. (2009), the authors compared state of art texture methods for leaf identification and the best results were achieved by them.

In all methods of extracting the AVS used the naive Bayes classification and the cross validation learning method were used. Each image processing, 80% of the images were used for training and 20% for testing "blind". The classification experiment was carried out considering the four levels of Ca deficiency. These levels were controlled and also validated with the chemistry analysis. The goal of the classification experiment is verifying the image analysis accuracy to detected the nutrient deficiency classifying the groups according both chemistry analysis and controlled level of Ca.

The VFD routines used works with binary images because it follows the proposal of Backes et al. (2009) in which the image signature is calculated for all reE values:

$$E = 1, \sqrt{2}, \sqrt{3}, \dots, r_{max} \quad (2)$$

$$\bar{U}(r_{max}) = [\log V(1), \log V(\sqrt{2}), \log V(\sqrt{3}), \dots, \log V(r_{max})] \quad (3)$$

Where, E is the set of Euclidean distances for a maximum radius r_{max} . In this routine the radius varied from 1 μm to 20 μm .

The transformed of Gabor bi-dimensional is a Gaussian function modulated in a senoidal oriented with a frequency and a direction, and its bi-dimensional form in the space and frequency is given by the following equations.

$$g(x, y) = \left(\frac{1}{2\pi\sigma_x\sigma_y} \right) \exp \left[-\frac{1}{2} \left(\frac{x^2}{\sigma_x^2} + \frac{y^2}{\sigma_y^2} \right) \right] + 2\pi jWx \quad (4)$$

$$G(u, v) = \exp \left\{ -\frac{1}{2} \left[\frac{(u-W)^2}{\sigma_u^2} + \frac{v^2}{\sigma_v^2} \right] \right\} \quad (5)$$

Where, frequency W and a direction θ , and its bi-dimensional form in the space $g(x,y)$ and frequency $G(u,v)$.

The transformed of Gabor can be adapted as a wavelet and in such a case these equations are used as a mother wallet. In the next step, a filter dictionary can be obtained by dilation and rotation of $gz(x,y)$ through the function generated as proposed by Manjunath and Ma (1996):

$$g_{mn}(x,y) = a^{-m} g(x', y') \quad (6)$$

Where, $a > 1$; m, n are the scale and orientation, respectively, with $m = 0, 1, \dots, M-1$ and $n = 0, 1, \dots, N-1$; M is the total number of scales and N is the total number of orientations.

2.7 Classification/Identification

Finally, the last part is the classification/identification, where the pattern recognition algorithms performance the classification of the leaves based on the feature vector extracted in the previous step.

For all methods the Naive Bayes classification and the cross validation learning method were used. For the evaluation, the samples were separated randomly into n groups of roughly equal size and was made "to let an outside group" the cross-validation which can also be called a "n-fold cross-validation" test scheme. Samples were independent for each class, and these samples did not appear in the same training and testing. In each processing, 80% of the images were used for training and 20% for testing "blind".

For the best recognition result of Ca deficiency by the methods of AVS, the confusion matrices were generated to assess the amount of right classifications made by AVS. And it is important to know classes that were difficult to classify. In addition, were assessed the percentage of images correctly classified or Global Percentage of Right (GPR) and Kappa index (K).

The Kappa index indicates the correlation between GPR and truth. And Kappa index is evaluated as follows: 0.00-0.20: not trust; 0.21-0.40: low; 0.41-0.60: moderate; 0.61-0.80: trust; 0.81-1.00: worthy trust (Everitt & Dunn,

2001). The Kappa index is statistical measure of agreement or accuracy well know in pattern recognition (Congalton, 1991). The Kappa index is used in this study to measure the confidence of the classification.

3. Results

3.1 Calcium Concentration in NL and IL

In all three stages investigated, the increase of Ca in NL and IL was concurrent and significant ($p < 0.01$) with the Ca concentration in the nutrient solution. The IL fit a linear model (Figure 2a) and NL a quadratic model (Figure 2b). The symptoms were apparent when Ca was suppressed or in present in small concentrations (33%). In the present study, plants suppressed of Ca had the smallest concentration of this element both in IL and NL in all stages (Figure 2). As the Ca concentration increased in the nutrient solution, the concentration in leaves increased from 0.98 to 8.11 g.kg⁻¹ of Ca in IL and from 0.42 to 2.44 g.kg⁻¹ of Ca in NL.

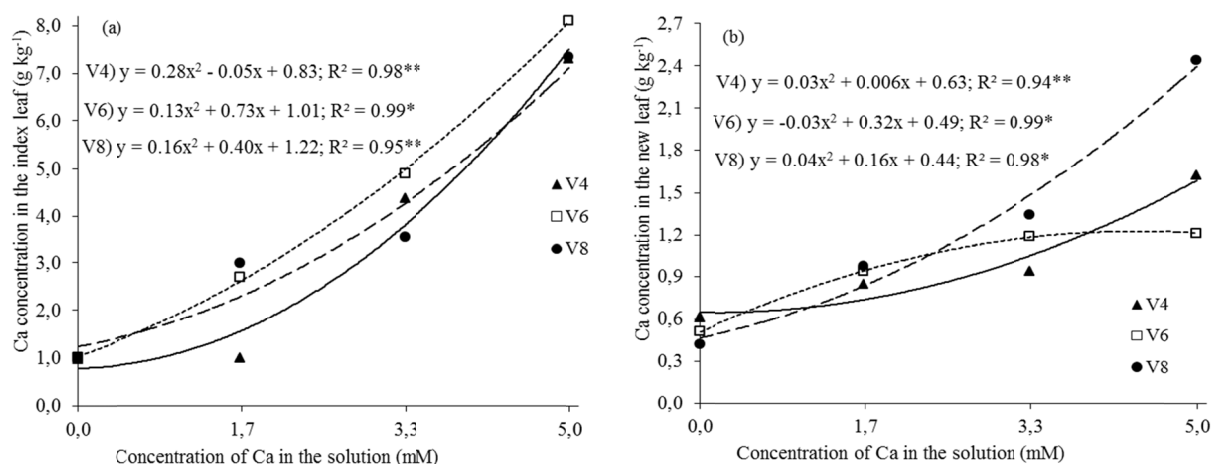


Figure 2. Concentration of calcium (Ca) in the index leaf (IL) (a) and new leaf (NL) (b) of maize (*Zea mays* L.) at the V4, V6 and V8 stages as a function of Ca concentration in nutrient solution. ******Significative at 1% and *****Significative at 5%

3.2 Visual Symptoms and Dry Mass of Shoots and Roots

In plants where Ca was completely suppressed, there was a massive decrease in growth, necrosis in the growth apex of leaves, evolving to the typical descent death. Therefore, we considered that the low Ca levels in nutrient solution caused the typical symptoms of Ca deficiency and allow the use of the images as standards for Ca deficiency identification through AVS. The dry mass production in shoots and roots were significantly different ($p < 0.01$) as Ca supply varied, fitting a quadratic model in all stages (Figure 3).

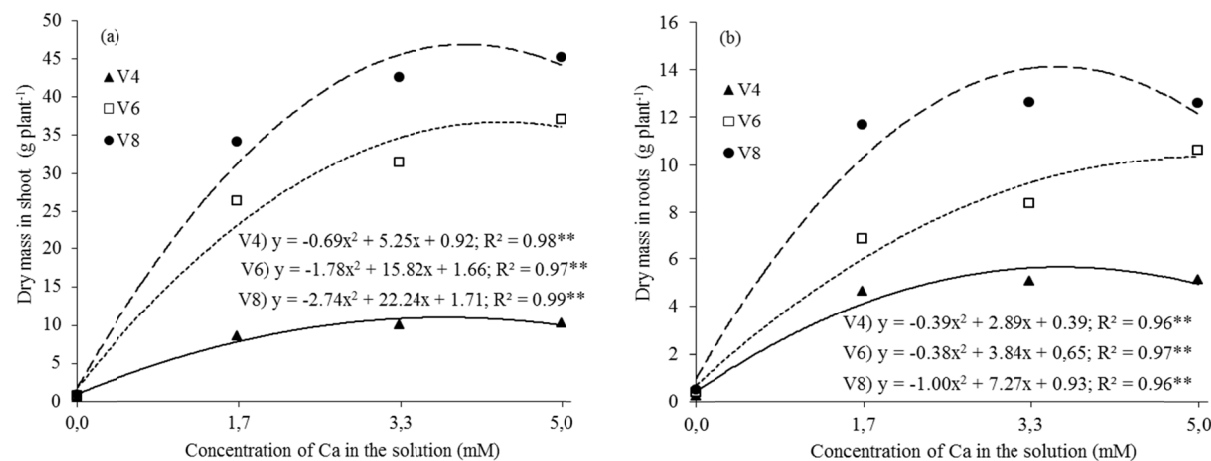


Figure 3. Dry mass in shoot (a) and dry mass in roots (b) of maize (*Zea mays* L.) at the V4, V6 and V8 stages as a function of calcium (Ca) concentration in nutrient solution. ******Significative at 1%

The symptoms of Ca deficiency appears first in the new leaves and meristems of maize (Figure 3). Morphological symptoms of Ca deficiency were observed in all plants with complete or partial lack of Ca in the nutrient solution, such as deformed leaves, with crisped margins thin and twisted tops (Figure 4).

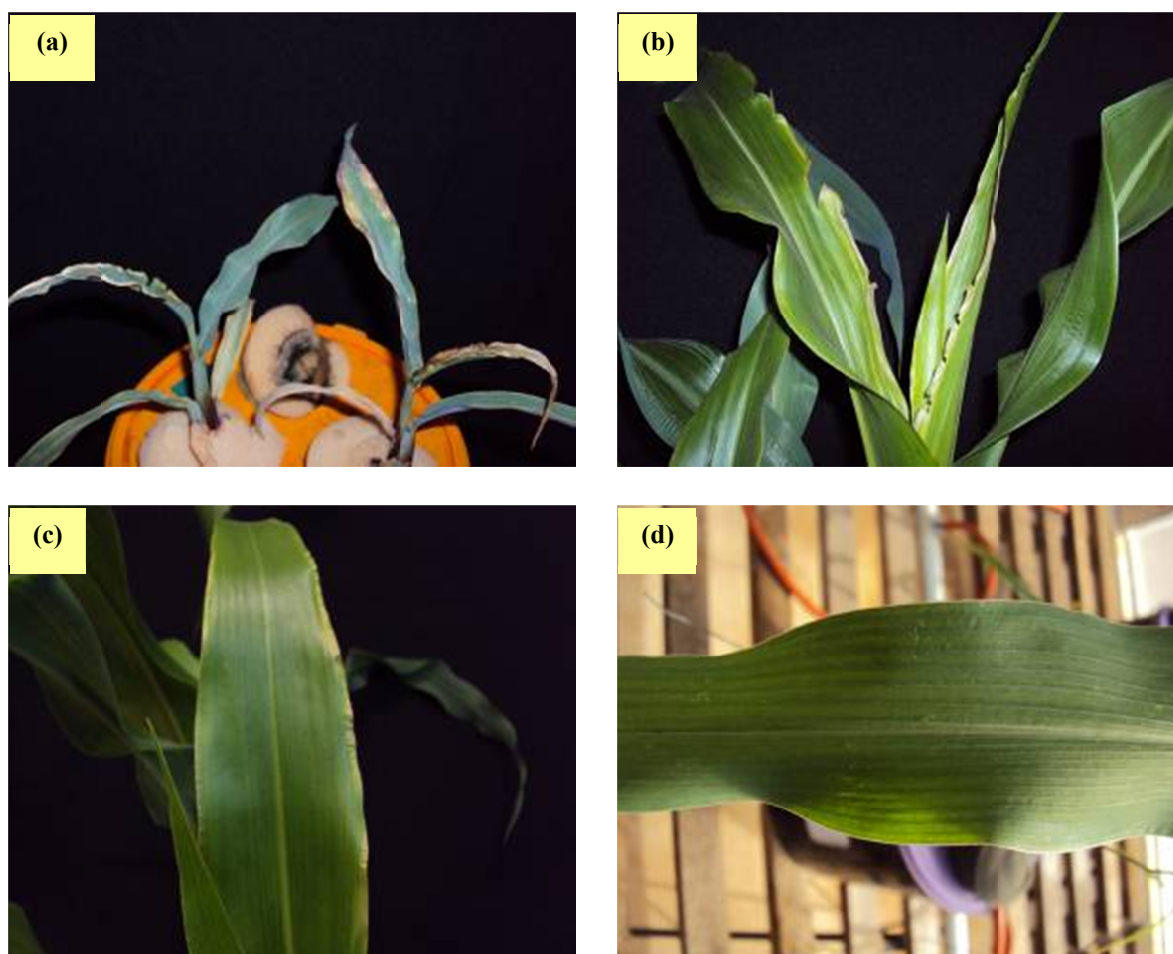


Figure 4. Dead maize meristem of maize grown into 0.0 mM Ca solution (a); Intense dilacerations of leaf margin in new leaves of maize grown into 1.7 mM of Ca (b); Margin deformation of leaves of maize grown into 3,4 mM Ca solution (c); and new maize leaf grown in nutrient solution without Ca deficiency (d), at the 29th day after emergence.

3.3 Artificial Visual System (AVS)

The best result of the AVS using gray scale images was the VFDC, with 69.0% of rights on the medium portion of the NL during the V4 stage, 66.0 % at the top portion of the leaves in V6 and 59% in the medium portion of IL in V8 (Table 1). The use of color images improve the percentage of rights (Table 2). In all growth stages the best results were found in NL using the GWE routine, reaching 80.0% and 69.5 % of rights in the medium portion during the V4 and V6 stages, and 65.0% at the leaf base during V8, and the Kappa was considered “very reliable”.

The best result was 80.0 % of rights in V4 (Kappa = 0.941), resulting that the GWE routine using color images has the best potential. In addition, the number of rights were high in V4 and decreased towards the V8, meaning that the routine is suitable to identify Ca deficiency in young plants.

The NL is the leaf that had more information recovered by the AVS regarding the Ca nutritional status of maize plants grown in greenhouse (Table 2). The confusion matrix is shown in Table 3 related to the GWE method in the medium portion of the NL during the V4. From 50 images analyzed, for the 0.0 nM of Ca solution, 98% of images were correctly classified, and the other 2% were classified as being grown in the 1.7 mM of Ca solution. The “zero” at the end of lines means there was no image classified as being of 3.3 mM or 5.0 mM Ca solutions. In the class of leaves that were grown in 1.7 mM of Ca, 66% of images were correctly classified, 30% of images were classified as being grown in 3.3 mM and 4% as 0.0 mM.

Table 1. Global percentage of rights (GPR) of gray scale images using the volumetric fractal dimension (VFD), volumetric fractal dimension with canonical analysis (VFDCA), and Gabor wavelets (GW) to assess leaf calcium (Ca), and corresponding Kappa index (K), for the top, middle and bottom sections of the index leaf and new leaf for the same sections from maize plants (*Zea mays* L.) at the V4, V6 and V8, under four levels of Ca in nutrient solution in greenhouse

		IL						NL					
		VFD		VFDCA		GW		VFD		VFDCA		GW	
		GPR	Kappa	GPR	Kappa	GPR	Kappa	GPR	Kappa	GPR	Kappa	GPR	Kappa
V4	Top	34.0	0.590	55.0	0.770	46.5	0.718	41.5	0.695	66.0	0.866	51.5	0.765
	Base	29.5	0.557	49.5	0.741	44.5	0.686	39.5	0.65	62.5	0.858	52.5	0.764
	Middle	21.5	0.473	53.5	0.769	39.0	0.639	39.5	0.647	69.0	0.879	60.0	0.844
V6	Top	45.5	0.681	51.0	0.733	48.5	0.742	39.0	0.604	66.0	0.867	59.9	0.810
	Base	46.5	0.724	46.0	0.707	48.0	0.719	35.0	0.571	65.5	0.857	57.5	0.812
	Middle	44.0	0.702	48.0	0.740	45.5	0.690	32.0	0.539	55.5	0.798	57.0	0.788
V8	Top	48.5	0.741	54.0	0.794	50.5	0.785	48.5	0.708	53.5	0.795	54.0	0.780
	Base	50.5	0.734	58.5	0.788	52.5	0.749	48.0	0.698	55.0	0.783	54.5	0.768
	Middle	55.5	0.747	59.0	0.795	55.0	0.767	51.0	0.707	52.0	0.797	43.0	0.742

Table 2. Global percentage of rights (GPR) of colors images using the volumetric fractal dimension (VFD), volumetric fractal dimension with canonical analysis (VFDCA), and Gabor wavelets (GW) to assess leaf calcium (Ca), and corresponding Kappa index (K), for the top, middle and bottom sections of the index leaf and new leaf for the same sections from maize plants (*Zea mays* L.) at the V4, V6 and V8, under four levels of Ca in nutrient solution in greenhouse

		FI						FN					
		VFD		VFDCA		GW		VFD		VFDCA		GW	
		GPR	Kappa	GPR	Kappa	GPR	Kappa	GPR	Kappa	GPR	Kappa	GPR	Kappa
V4	Top	46.5	0.722	60.0	0.79	55.5	0.771	43.0	0.719	67.5	0.873	62.5	0.854
	Base	40.0	0.622	35.5	0.633	50.5	0.773	54.0	0.768	71.0	0.89	60.5	0.859
	Middle	42.5	0.7	54.5	0.778	55.5	0.793	42.0	0.698	65.5	0.873	80.0	0.941
V6	Top	48.5	0.716	49.5	0.762	53.0	0.780	47.0	0.686	48.5	0.745	62.5	0.867
	Base	48.0	0.738	60.0	0.829	61.0	0.810	45.5	0.704	51.0	0.734	67.0	0.896
	Middle	47.0	0.691	52.5	0.742	56.0	0.789	39.5	0.668	48.5	0.700	69.5	0.901
V8	Top	56.5	0.795	55.0	0.784	58.5	0.807	51.0	0.726	43.5	0.708	64.5	0.808
	Base	52.5	0.781	58.0	0.827	59.5	0.820	42.0	0.703	49.0	0.742	65.0	0.849
	Middle	51.5	0.767	55.0	0.795	62.5	0.814	55.5	0.769	48.5	0.734	57.5	0.813

Table 3. Confusion matrix of the medium portion of maize new leaves (NL), classified by the Gabor Wavelets Energy (GWE) on color images of stage V4 leaves, submitted to calcium (Ca) levels in nutrient solution

Correct classification	% images classified using the GWE of NL in V4 with color images			
	0.0 mM	1.7 mM	3.3 mM	5.0 mM
0.0 mM	98	2	0	0
1.7 mM	4	66	30	0
3.3 mM	0	26	72	2
5.0 mM	6	2	8	84

Another interesting aspect of the confusion matrix is the percentage of rights for the 0.0 mM and 3.3 mM. The results point to the 0.0 mM as being the easiest to classify, and that the greatest percentage of errors occurs in the 3.3 mM (Table 3). This probably happens because the images obtained from the leaves grown into the 3.3 mM solution are very close to those of leaves grown into the 1.7 mM. Even though, the AVS still can correctly classify a large amount of images. This happens because the Ca concentration in the NL of V4 plants grown into the 3.3 mM is 0.94 g kg⁻¹ (Figure 2b) and are very close to the Ca concentration in the NL of V4 plants grown into the 1.7 mM of Ca solution, which is 0.85 g kg⁻¹ of Ca (Figure 2b). Such closeness may have caused the difficulty of the AVS to identify the nutritional status of plants. However, the discrimination among the Ca levels is still reasonable,

since it would be nearly impossible to distinguish visual symptoms in plants with Ca levels this close to each other. The AVS was able to identify Ca severe (0.0 mM) and moderate (1.7 mM) deficiencies, when the deficiency is to small (3.3 mM), the percentage of rights is 80%. Therefore, it would be possible to correct deficiency even at very small levels, but still causes decrease in the crop production.

4. Discussion

The results of Ca concentration in NL and IL are in accord with those reported by Silveira and Monteiro (2010) in their study of N and Ca nutrition of Tanzania grass, where the isolated effect of Ca concentration in recently expanded leaves fit a quadratic model. The concentration of Ca in the IL was greater as compared to the NL because Ca is usually immobile, therefore the Ca deficiency symptoms appears firstly in the newer leaves (Malavolta, 2006). Grangeiro et al. (2006) also stated that Ca inside the plant moves together with water and once deposited, do not show relocation towards other plant tissues, being accumulated mainly in tissues with intense transpiration. According to Malavolta (2006), the amount of Ca transfer through phloem is very small, resulting in Ca deficiency symptoms to appear first in new leaves.

The visual symptoms of Ca deficiency in NL agrees with Ramos et al. (2009). According to Epstein & Bloom (2006), Ca demand seems to be intense in such tissues and Ca in older tissues is not relocates to younger tissues. The small mobility of Ca is mainly due to the low solubility forms it assumes inside plants, such as the pectate of the medium lamellae of cell wall, which makes plant requirement of Ca be constant along its growth (Malavolta, 2006). The visual symptoms are in accordance with previous reports (Taiz & Zeiger, 2010; Epstein & Bloom, 2006; Epstein, 1975). Malavolta (2006) reported such symptoms, and according to Mengel and Kirkby (1987), the requirement of Ca by maize can be easily demonstrated by interrupting the supply to the plant roots and observing the immediate decrease in growth. According to Marschner (2011), Ca deficiency usually retards the plant growth. Mengel and Kirkby (1987) states the need of Ca for plant growth is easily demonstrated by the interruption of Ca supply to roots.

According to Patrício and Riederb (2018) computer vision systems are already widely employed in different segments of agricultural production and they can be used in grading systems for maize. The use of such systems provides a simple, producing accurate descriptive data.

Baesso et al. (2020), Luz et al. (2018), Romualdo et al. (2018), Silva et al. (2014), Romualdo et al. (2014), compared state of art texture methods for leaf identification of nutrition maize plants.

Studying the identification of Mg concentrations in maize by AVS, Silva et al. (2014) also found that the analysis of color images scored higher than gray images in all stages of development of the plant and then the AVS identified the images of the leaves of corn with levels of Mg with 75.5% rights using the middle section of the IL by the VFDCA technique, based on color images in V4 stage.

Romualdo et al. (2014) studying nitrogen nutritional status in maize plants, found percentage of right of 82.5% using Gabor Wavelet technique, as in this study in which the percentage of rights is 80% in V4 stage. Romualdo et al. (2018) found accuracy rate for nitrogen patterns was 80% at V4 stage using spectral indexes for identification of nitrogen deficiency in maize.

In study de boron deficiency identification on maize, the best method texture image analysis was Fractal and achieved 88.75% of accuracy in V4 stage; Gabor has already reached 81.75% of accuracy in differentiating (Luz et al., 2018). Baesso et al. (2020) found a 66% of rights for nutritional diagnosis of maize with calcium silicate and magnesium.

Through these systems it is possible to automate laborious tasks, in a non-destructive way, producing adequate data, bringing gains of production, quality, and food security (Patrício & Riederb, 2018).

5. Conclusion

Maize plants grown into greenhouse show visual symptoms related to Ca deficiency, which significantly interfere in shoot and root dry mass production. The NL of maize is the leaf that has the greatest amount of information for the AVS classification using color images. IN color images, the best routine to identify Ca deficiency was the GWE. The AVS had 80% of rights in identifying Ca deficiency in color images, with a Kappa of 0.941 “very reliable”. This was superior to all gray scale images in all growth stages studied.

References

- Amaral Filho, J. P. R., Fornasieri Filho, D., Farinelli, R., & Barbosa, J. C. (2005). Row spacing, population density and nitrogen fertilization in maize. *Revista Brasileira de Ciência do Solo*, 29, 467-473. <https://doi.org/10.1590/S0100-06832005000300017>

- Backes, A. R. D., Casanova, D., & Bruno, O. M. (2009). Plant leaf identification based on volumetric fractal dimension. *International Journal of Pattern Recognition and Artificial Intelligence*, 23, 1145-1160. <https://doi.org/10.1142/S0218001409007508>
- Backes, A. R., & Bruno, O. M., (2013). Texture analysis using volume-radius fractal dimension. *Applied Mathematics and Computation*, 219, 5870-5875. <https://doi.org/10.1016/j.amc.2012.11.092>
- Baesso, M. M., Aprilanti, T. M. G., Modolo, A. J., & Rossi, F. (2020). Artificial vision for nutritional diagnosis of corn grown with calcium silicate and magnesium in ponderal doses and high dilutions. *Brazilian Journal of Biosystems Engineering*, 14, 36-47. <https://doi.org/10.18011/bioeng2020v14n1p36-47>
- Baesso, M. M., Pinto, F. A. C., Queiroz, D. M., Vieira L. B., & Alves, E. A. (2007). Determination of nitrogen status in bean plants using color digital images. *Engenharia Agrícola*, 27, 520-528. <https://doi.org/10.1590/S0100-69162007000300022>
- Baesso, M. M., Varella, C. A., Martins, G. A., Modolo, A. J., & Brandelero, E. M. (2012). Determination of nutritional deficiency level of nitrogen in bean using artificial neural networks. *Engenharia na Agricultura*, 20, 512-518. <https://doi.org/10.13083/1414-3984.v20n06a03>
- Bataglia, O. C., Furlani, A. M. C., Teixeira, J. P. F., Furlani, P. R., & Gallo, J. R. (1983). *Métodos de análises química de plantas* (Boletim Técnico 78, p. 48). Instituto Agronômico, Campinas.
- Bruno, O. M. (2000). *Paralelismo em Visão Natural e Artificial* (Tese, Instituto de Física de São Carlos, Universidade de São Paulo, São Carlos).
- Casanova, D., Mesquita Sa Junior, J. J., & Bruno, O. M. (2009). Plant leaf identification using Gabor wavelets. *International Journal of Imaging Systems and Technology*, 19, 236-243. <https://doi.org/10.1002/ima.20201>
- Congalton, R. G. (1991). A review of assessing the accuracy of classifications of remotely sensed data. *Remote Sensing of Environment*, 37, 35-46. [https://doi.org/10.1016/0034-4257\(91\)90048-B](https://doi.org/10.1016/0034-4257(91)90048-B)
- Epstein, E. (1975). *Nutrição mineral das plantas: Princípios e perspectivas* (p. 341). Tradução e notas de Eurípedes Malavolta. Livros Técnicos e Científicos Editora S.A. and Editora da Universidade de São Paulo, São Paulo.
- Epstein, E., & Bloom, A. J. (2006). *Mineral nutrition of plants: Principles and perspectives* (2nd ed., p. 380). Sunderland: Sinauer Associates.
- Everitt, B. S., & Dunn, G. (2001). *Applied multivariate data analysis* (2nd ed., p. 342). London: Arnold, London. <https://doi.org/10.1002/9781118887486>
- Fancelli, A. L. (1986). *Plantas alimentícias: Guia para aula, estudo e discussão* (p. 131). Centro Acadêmico “Luiz de Queiroz”, Piracicaba.
- FAO (Food and Agriculture Organization of the United Nation). (2022). Retrieved from <http://faostat3.fao.org>
- Florindo, J. B., Silva, N. R., Romualdo, L. M., Silva, F. F., Luz, P. H. C., Herling, V. R., & Bruno, O. M. (2014). Brachiaria species identification using imaging techniques based on fractal descriptors. *Computers and Electronics in Agriculture*, 103, 48-54. <https://doi.org/10.1016/j.compag.2014.02.005>
- Gonzalez, R. C., & Woods, R. E. (2007). *Digital Image Processing* (3rd ed., p. 528). Pearson.
- Grangeiro, L. C., Costa, K. R., Medeiros, M. A., Salviano, A. M., Negreiros, M. Z., Bezerra Neto, F., & Oliveira, S. L. (2006). Accumulation of nutrients by three lettuce cultivars grown under Semi-arid conditions. *Horticultura Brasileira*, 24, 190-194. <https://doi.org/10.1590/S0102-05362006000200013>
- Hoagland, D. R., & Arnon, D. I. (1950). *The water culture method for growing plants without soils* (p. 347). Berkeley: California Agricultural Experimental Station.
- Karcher, D. E., & Richardson, M. D. (2003). Quantifying turfgrass color using digital image analysis. *Crop Science*, 43, 943-951. <https://doi.org/10.2135/cropsci2003.0943>
- Lukina, E. V., Freeman, K. W., Wynn, K. J., Thomason, W. E., Mullen, R. W., Stone, M. L., ... Raun, W. R. (2001). Nitrogen fertilization optimization algorithm based on in-season estimates of yield and plant nitrogen uptake. *Journal of Plant Nutrition*, 24, 885-898. <https://doi.org/10.1081/PLN-100103780>
- Luz, P. H. C., Marin, M. A., Devechio, F. F. S., Romualdo, L. M., Zuñiga, A. M. G., Oliveira, M. W. S., ... Bruno, O. M. (2018). Boron deficiency precisely identified on growth stage V4 of maize crop using texture image analysis. *Communications in Soil Science and Plant Analysis*, 49, 159-169. <https://doi.org/10.1080/00103624.2017.1421644>

- Malavolta, E. (2006). *Manual de nutrição de plantas* (p. 638). Agronômica Ceres, São Paulo.
- Manjunath, B. S., & Ma, W. Y. (1996). Texture features for browsing and retrieval of image data. *IEEE Transactions on Pattern Analysis and Machine Intelligence*, 18(8), 837-842. <https://doi.org/10.1109/34.531803>
- Marschner, P. (2011). *Mineral nutrition of higher plants* (3rd ed., p. 672). Academic Press, London.
- Mengel, K., & Kirkby, E. (1987). *Principles of plant nutrition* (p. 687). International Potash Institute, Bern.
- Patrício, D. I., & Riederb, R. (2018). Computer vision and artificial intelligence in precision agriculture for grain crops: A systematic review. *Computers and Electronics in Agriculture*, 153, 69-81. <https://doi.org/10.1016/j.compag.2018.08.001>
- Punam, K. S., & Udupa, J. K. (2001). Optimum image thresholding via class uncertainty and region homogeneity. *IEEE Transactions on Pattern Analysis and Machine Intelligence*, 23, 689-706. <https://doi.org/10.1109/34.935844>
- Rambo, L., Silva, P. R. F., Argenta, G., & Sangoi, L. (2004). Plant parameters to refine the management of nitrogen side-dress application in maize. *Ciência Rural*, 34, 1637-1645. <https://doi.org/10.1590/S0103-84782004000500052>
- Ramos, M. J. M., Monnerat, P. H., Carvalho, A. J. C., Pinto, J. L. A., & Silva, J. A. (2009). Visual symptoms of macronutrients and boron deficiency in 'imperial' pineapple. *Revista Brasileira de Fruticultura*, 31, 252-256. <https://doi.org/10.1590/S0100-29452009000100035>
- Reis, A. R., Furlani Junior, E., Buzetti, S., & Andreotti, M. (2006). Metodologia e técnicas experimentais diagnóstico da exigência do cafeeiro em nitrogênio pela utilização do medidos portátil de clorofila. *Bragantia*, 65, 163-171. <https://doi.org/10.1590/S0006-87052006000100021>
- Romualdo, L. M., Luz, P. H. C., Baesso, M. M., Devechio, F. F. S., & Bet, J. A. (2018). Spectral indexes for identification of nitrogen deficiency in maize. *Revista Ciência Agronômica*, 49, 183-191. <https://doi.org/10.5935/1806-6690.20180021>
- Romualdo, L. M., Luz, P. H. C., Devechio, F. F. S., Marin, M. A., Zúñiga, A. M. G., Bruno, O. M., & Herling, V. R. (2014). Use of artificial vision techniques for diagnostic of nitrogen nutritional status in maize plants. *Computers and Electronics in Agriculture*, 104, 63-70. <https://doi.org/10.1016/j.compag.2014.03.009>
- Rossatto, D., Casanova, D., Kolb, R., & Bruno, O. M. (2011). Fractal analysis of leaf-texture properties as a tool for taxonomic and identification purposes: A case study with species from Neotropical Melastomataceae (*Miconieae* tribe). *Plant Systematics and Evolution*, 291, 103-116. <https://doi.org/10.1007/s00606-010-0366-2>
- Silva, F. F., Luz, P. H. C., Romualdo, L. M., Marin, M. A., Zúñiga, A. M. G., Herling, V. R., & Bruno, O. M. (2014). A diagnostic tool for magnesium nutrition in maize based on image analysis of different leaf sections. *Crop Science*, 54, 738-745. <https://doi.org/10.2135/cropsci2013.03.0165>
- Silveira, C. P., & Monteiro, F. A. (2010). Macronutrients concentrations in Tanzania guineagrass diagnostic leaves supplied with nitrogen and calcium rates. *Revista Brasileira de Zootecnia*, 39, 736-745. <https://doi.org/10.1590/S1516-35982010000400006>
- Steel, R. G. D., Torrie, J. H., & Dickey, D. A. (1997). *Principles and procedures of statistics. A Biometrical Approach* (3rd ed., p. 666). McGraw Hill Co, New York.
- Taiz, L., & Zeiger, E. (2010). *Plant Physiology* (5th ed., p. 782). Sinauer Associates, Sunderland.
- Wu, J., Wang, D., Rosen, C. J., & Bauer, M. E. (2007). Comparison of petiole nitrate concentrations, SPAD chlorophyll readings, and QuickBird satellite imagery in detecting nitrogen status of potato canopies. *Field Crops Research*, 101, 96-103. <https://doi.org/10.1016/j.fcr.2006.09.014>

Copyrights

Copyright for this article is retained by the author(s), with first publication rights granted to the journal.

This is an open-access article distributed under the terms and conditions of the Creative Commons Attribution license (<http://creativecommons.org/licenses/by/4.0/>).